Mem. S.A.It. Suppl. Vol. 19, 302

Memorie della
Supplementi

Central dark matter trends in early-type galaxies

C. Tortora[1], N.R. Napolitano[2], A.J. Romanowsky[3], and Ph. Jetzer[1]

[1] Universität Zürich, Institut für Theoretische Physik, Winterthurerstrasse 190, CH-8057, Zürich, Switzerland e-mail: ctortora@physik.uzh.ch

[2] INAF – Osservatorio Astronomico di Capodimonte, Salita Moiariello, 16, 80131 - Napoli, Italy

[3] UCO/Lick Observatory, University of California, Santa Cruz, CA 95064, USA

Abstract. We analyze the correlations between the central dark matter content of early-type galaxies and their sizes and ages, using a sample of intermediate-redshift ($z \sim 0.2$) gravitational lenses from the SLACS survey, and by comparing them to a larger sample of $z \sim 0$ galaxies. For a given stellar mass, we find that for galaxies with larger sizes, the DM fraction increases and the mean DM density decreases, consistently with the cuspy halos expected in cosmological formation scenarios. The DM fraction also decreases with stellar age, which can be partially explained by the inverse correlation between size and age. The residual trend may point to systematic dependencies on formation epoch of halo contraction or stellar initial mass functions.

Key words. dark matter – gravitational lensing – galaxies : evolution.

1. Introduction

The mass content of early-type galaxies' (ETGs) central regions has been extensively investigated (e.g., Gerhard et al. 2001; Cappellari et al. 2006; Tortora et al. 2009, T+09, hereafter), with building evidence that the central dark matter (DM) fraction ($f_{\rm DM}$) is an increasing function of the total stellar mass ($M_{\star}$), providing the main driver for the tilt of the fundamental plane (e.g., T+09).

New insights into the galaxy assembly process are emerging from joint analyses of the structural and star formation properties of nearby ETGs (e.g., Gargiulo et al. 2009; Graves & Faber 2010; Napolitano, Romanowsky & Tortora 2010, NRT10 hereafter). A key discovery of NRT10 is an anti-correlation between $f_{\rm DM}$ and the galaxy stellar age, such that older galaxies (at a fixed $M_{\star}$) have lower $f_{\rm DM}$. In the context of ΛCDM halos, this trend can be partially explained by an anti-correlation between galaxy sizes and ages, with the remaining effect apparently driven by variations in star formation efficiency, stellar initial mass function (IMF), or DM distribution (e.g., adiabatic contraction, AC hereafter). As discussed in NRT10, such correlations would have deep implications for the assembly histories of ETGs, but critically need to be confirmed by independent analyses. Gravitational lenses offer a unique tool to map the mass profile in galaxies over a range of redshifts. Here, we will use the SLACS sample data (Auger et al. 2009, A+09, hereafter) to extend the analysis of NRT10, using both lensing and dynamics as independent probes of total mass, and pro-

Send offprint requests to: C. Tortora

viding a higher-redshift ($z \sim 0.2$) comparison to the $z \sim 0$ galaxies previously studied[1]. For further details, also check Tortora et al. (2010, T+10 hereafter).

2. Data sample and analysis

The lensing galaxy sample is taken from the SLACS survey (A+09), and consists of 66 galaxies (see T+10), with a lens galaxy redshift (z_l) in the range $0.05 \leq z_l \leq 0.5$, and a median of $z_l \sim 0.2$. As a $z \sim 0$ comparison sample, we use the collection of 330 ETGs over the same mass range analyzed in T+09 and NRT10.

To estimate stellar mass-to-light ratios ($\Upsilon_\star$) and star formation histories, we use a set of synthetic spectra from Bruzual & Charlot (2003), which we fit to the SDSS photometry. A Kroupa (2001) IMF is assumed.

We derive the deprojected total mass from dynamics and lensing observables, and separate the DM from the stellar components using the stellar mass estimates discussed in the previous section. We adopt the stellar effective radius $R_{\rm eff}$ as the fiducial reference point for mass comparisons. In both galaxy samples, the mass constraints are generally based on measurements at smaller radii, and therefore some extrapolation is required. For the total mass distribution we adopt a singular isothermal sphere (SIS) with density $\rho(r) = \sigma^2_{\rm SIS}/(2\pi G r^2)$, where $\sigma_{\rm SIS}$ is an unknown normalization to be determined by fitting the observables. For the stars, we adopt a constant-Υ_* mass profile based on the Hernquist (1990) model. To estimate dynamical masses we have used the SDSS stellar velocity dispersions $\sigma_{\rm SDSS}$, measured within a circular aperture of $R_{\rm ap} = 1.5''$. We have adopted the spherical Jeans equation to derive the surface brightness weighted velocity dispersion $\sigma_{\rm ap,SIS}$ within $R_{\rm ap}$, to be matched to $\sigma_{\rm SDSS}$. For the lensing mass estimates, we have used the Einstein radius $R_{\rm E}$, to derive a model independent measurement of projected mass ($M_{\rm proj}$) within $R_{\rm E}$, Finally we match the prediction of the SIS model projected mass, $M_{proj,SIS}$ with M_E to have a further constraint on the only free model parameter for each galaxy, $\sigma_{\rm SIS}$. To estimate the 3D deprojected mass profile (which we extrapolate to $r = R_{\rm eff}$ to obtain our reference mass values), we adopt a combination of the constraints for our final masses, by minimizing with respect to $\sigma_{\rm SIS}$ a combined χ^2 function including one term for dynamics and one for lensing observables.

We will focus on the central deprojected $f_{\rm DM}$ and the mean DM density within $R_{\rm eff}$, defined as $\langle\rho_{\rm DM}\rangle = M_{\rm DM}/(4\pi {R_{\rm eff}}^3/3)$ where $M_{\rm DM} = M_{\rm tot} - M_\star$ at $R_{\rm eff}$ is the DM mass.

As in T+09 and NRT10, to interpret the observational results, we construct a series of toy mass models based on ΛCDM cosmological simulations. For each bin in $M_\star$, we use the average $R_{\rm eff}$-age relations from the combined lens+local sample, and parameterize the virial DM mass by a star formation efficiency $\epsilon_{\rm SF} = M_\star/(\Omega_{\rm bar} M_{\rm tot})$, where $\Omega_{\rm bar} = 0.17$ (Spergel et al. 2007) is the baryon density parameter. The halo densities are initially characterized as Navarro et al. (1997) profiles following an average mass-concentration relation, adjusted by $(1+z)^{-1}$ for the lens galaxies. A recipe for AC from baryon settling is then applied (Gnedin et al. 2004).

3. Results: correlations with size and formation epoch

In order to marginalize any correlations with $M_\star$, we group the galaxies from both samples into bins of common median mass: $\log M_*/M_\odot \sim 11.6, 11.3$ and 10.9.

Fig. 1 demonstrates that there is a strong positive correlation between $f_{\rm DM}$ and $R_{\rm eff}$, once the galaxies are divided into mass bins. This may be understood as a larger $R_{\rm eff}$ enclosing a bigger portion of the DM halo; this "aperture effect" appears to be more dominant than the $f_{\rm DM}$ correlation with $M_\star$. The local and lens samples appear reasonably similar, although the lens galaxies in the lowest mass bin are systematically higher, which is an issue we will discuss below. Both samples are in rough agreement with our ΛCDM toy model predictions (top panel). We have also derived that the average DM density $\langle\rho_{\rm DM}\rangle$ strongly anti-

[1] In the paper, we use a cosmological model with $(\Omega_m, \Omega_\Lambda, h) = (0.3, 0.7, 0.7)$, where $h = H_0/100\,{\rm km\,s^{-1}\,Mpc^{-1}}$ (Spergel et al. 2007).

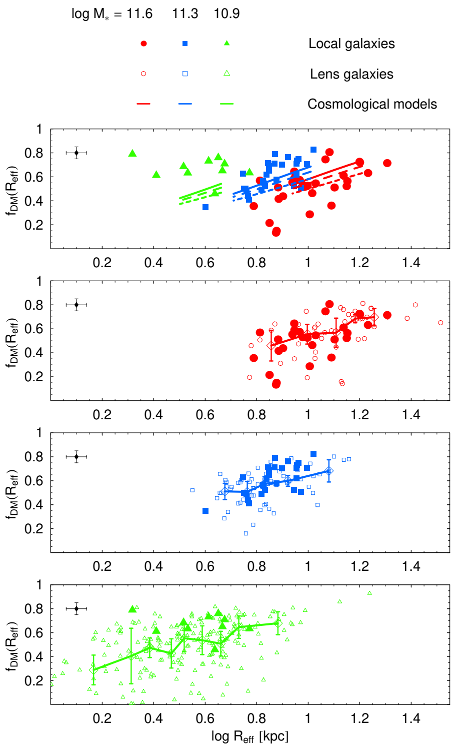

Fig. 1. Dark matter fraction within an effective radius ($R_{\rm eff}$) as a function of $R_{\rm eff}$. The lens and local galaxies are shown as filled and open symbols, respectively. For the latter, open symbols with error bars show the median and ±25% values. Typical 1σ uncertainties for individual galaxies are shown to the left. The differently colored symbols denote different bins of stellar mass, as labeled in the legend on the top. The second panel from the top shows the combined bins for the lens galaxies only and includes toy-model ΛCDM predictions: solid, long-dashed, and short-dashed curves show star formation efficiencies of $\epsilon_{\rm SF} = 0.03, 0.1, 0.3$, respectively.

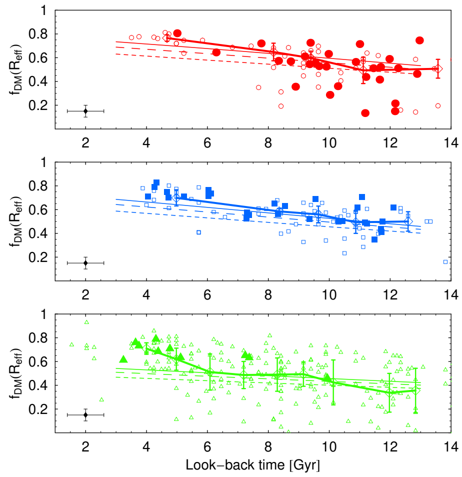

Fig. 2. DM fraction within 1 $R_{\rm eff}$ as a function of the galaxy stellar "age". See Figs. 1 for the meaning of symbols.

correlates with $R_{\rm eff}$ and are substantially larger than those of local spirals, implying different formation mechanisms. The implication is that we are measuring a mean DM density profile with radius, with a best fitted log slope of ~ -1.7. As discussed in NRT10, this steep slope is indicative of cuspy halos, perhaps as induced by AC (T+10).

Finally, we consider the $f_{\rm DM}$-age dependencies in Fig. 2, again using separate $M_\star$ bins[2]. The lens and local galaxies match up remarkably well in general, showing a clear trend for lower $f_{\rm DM}$ at older ages. At a fixed galaxy age and mass, the higher-z sample does not show any significant difference with the local galaxies. Since we have not applied any evolutionary corrections, the implication is that in the last ~ 2.5 Gyr (on average) the galaxy populations have experienced no measurable evolution except stellar aging. We also include the ΛCDM toy models in Fig. 2, and see that some $f_{\rm DM}$-age anticorrelation is expected, which can be traced to the anti-correlation between $R_{\rm eff}$ and age. However, there are indications in every mass bin that the observed $f_{\rm DM}$-age slope is steeper than in the models. As discussed in NRT10, this could be due to the fact that AC is more effective in younger galaxies, or that older galaxies have "lighter" IMFs (e.g., Kroupa versus Salpeter 1955 for the younger galaxies).

[2] We adopt the look-back time to the formation epoch in order to put all the galaxies with different observed redshifts on a common reference frame.

4. Conclusions

We have analyzed the central DM content of a sample of intermediate-z lenses from the latest release of the SLACS survey (A+09). Following the phenomenological framework introduced in T+09 and NRT10 we have discussed scaling relations between DM fraction, galaxy size, and formation epoch. Gravitational lensing and dynamical analyses are used to constrain the total mass profile, while synthetic spectral populations are used to infer the stellar mass and other stellar properties such as galaxy age.

ETGs at $z \sim 0.2$ are found to be similar to local ones. The somewhat surprising findings of NRT10 are now confirmed with an independent and arguably more robust data set. The DM fraction within $R_{\rm eff}$ is found to strongly correlate with $R_{\rm eff}$, because larger length-scales probe a more DM dominated region. On these scales, the DM mean density decreases with $R_{\rm eff}$ as $\langle \rho_{\rm DM} \rangle \propto R_{\rm eff}{}^{-1.7}$, which argues for cuspy DM halos for ETGs out to $z \sim 0.5$. At a fixed stellar mass and length-scale, we have found that the DM halos of ETGs are denser than those of local spiral galaxies, providing a critical test for the merging formation scenario (see also Cardone & Tortora 2010). Finally, we have confirmed our earlier finding that central DM content anti-correlates with stellar age. The strength of this correlation appears to exceed what is expected from size-age effects. A fundamental connection between galactic structure and star formation history is implied, which we propose is a consequence of variations with formation epoch of either DM halo contraction or stellar IMF.

For the future, we plan to investigate the impact on these results of more complex total and DM galaxy profiles along the lines of recent work in Cardone et al. (2009) and Cardone & Tortora (2010). New high-quality data are also expected with the advent of future surveys both in the local Universe and at larger redshifts. Such surveys will include larger samples of gravitational lenses along with more detailed spectroscopic information, and could be used to verify and extend the results presented here, providing a clearer picture of the physical processes of ETG assembly.

Acknowledgements. CT was supported by the Swiss National Science Foundation. AJR was supported by National Science Foundation Grants AST-0808099 and AST-0909237.

References

Auger, M.W., Treu, T., Bolton, A. S., et al. 2009, ApJ, 705, 1099 (A+09)
Bruzual, A. G. & Charlot, S. 2003, MNRAS, 344, 1000
Cappellari, M., Bacon, R., Bureau, M. et al. 2006, MNRAS, 366, 1126
Cardone, V. F., Tortora, C., Molinaro, R., Salzano, V. 2009, A&A, 504, 769
Cardone V. F. & Tortora C. 2010, MNRAS, 409, 1570
Gargiulo, A., Haines, C. P., Merluzzi, P. et al. 2009, MNRAS, 397, 75
Gerhard, O., Kronawitter, A., Saglia, R. P., Bender, R. 2001, AJ, 121, 1936
Gnedin, O. Y., Kravtsov, A. V., Klypin, A. A., Nagai, D. 2004, ApJ, 616, 16
Graves, G. J., & Faber, S. M. 2010, ApJ, 717, 803
Grillo, C., Gobat, R., Lombardi, M., Rosati, P. 2009, A&A, 501, 461
Hernquist, L. 1990, ApJ, 356, 359
Kroupa P., 2001, MNRAS, 322, 231
Napolitano, N. R., Romanowsky, A. J., Coccato, L. et al. 2009, MNRAS, 393, 329
Napolitano N. R., Romanowsky A. J. & Tortora, C. 2010, MNRAS, 405, 2351 (NRT10)
Navarro, J. F., Frenk, C. S., & White, S. D. M. 1997, ApJ, 490, 493
Romanowsky, A. J., Strader, J., Spitler, L. R. et al. 2009, AJ, 137, 4956
Salpeter, E.E. 1955 ApJ, 121, 161
Spergel, D. N., Bean, R., Doré, O. et al. 2007, ApJS, 170, 377
Tortora, C. Napolitano, N. R., Romanowsky, A. J., Capaccioli, M., Covone, G. 2009, MNRAS, 396, 1132
Tortora, C., Napolitano, N. R., Romanowsky, A. J., Jetzer, P. 2010, ApJ, 721, L1 (T+10)